

Evidence for complete and partial surface renewal at an air-water interface

A. T. Jessup,¹ W. E. Asher,¹ M. Atmane,² K. Phadnis,¹ C. J. Zappa,³ and M. R. Loewen²

Received 1 May 2009; revised 9 July 2009; accepted 30 July 2009; published 27 August 2009.

[1] A wind-wave flume is used to determine the extent to which the thermal boundary layer (TBL) at a wind-forced air-water interface is completely renewed from below. We measure skin temperature, T_{skin} , radiometrically, temperature immediately below the TBL, $T_{subskin}$, using a temperature profiler, and net heat flux using the gradient flux technique. The T_{skin} probability density function, $p(T_{skin})$, and surface renewal time scale, τ , were measured using passive and active infrared imaging techniques, respectively. We find that the mean percentile rank of $T_{subskin}$ in $p(T_{skin})$ is 99.90, implying that complete surface renewal occurs. This result suggests an alternative to radiometric measurement of T_{skin} through the simple combination of an infrared camera and an *in situ* temperature sensor. Comparison of the temperature difference across the TBL to the expected cooling implies that a significant portion of events only partially renew the TBL. This result should impact efforts to improve air-sea transfer models. **Citation:** Jessup, A. T., W. E. Asher, M. Atmane, K. Phadnis, C. J. Zappa, and M. R. Loewen (2009), Evidence for complete and partial surface renewal at an air-water interface, *Geophys. Res. Lett.*, *36*, L16601, doi:10.1029/2009GL038986.

1. Introduction

[2] The temperature difference across the oceanic thermal boundary layer (TBL) plays a critical role in air-sea fluxes of heat and gas [Fairall *et al.*, 1996; Ward and Donelan, 2006] and the accuracy of satellite-based infrared (IR) sensors [Donlon *et al.*, 1999, 2002]. The TBL, which is $O(10^{-3})$ m thick, is called the skin layer and the surface temperature measured by an IR radiometer is the skin sea surface temperature, SST_{skin} . (We use the notation introduced by Donlon *et al.* [2002] and formalized by the GHRSS-PP [2005] report. For laboratory temperatures, we use T rather than SST .) SST_{skin} is typically 0.1–0.3 K less than the temperature immediately below the TBL, $SST_{subskin}$ [Katsaros, 1980]. In addition to this cool skin effect, a warm layer of several degrees difference across the first few meters can occur under strong solar heating and low winds [Donlon *et al.*, 2002; Fairall *et al.*, 1996; Ward, 2006].

[3] Except under quiescent conditions, the skin layer is continually disrupted by turbulent eddies and breaking waves. Thus the skin layer is in a constant cycle of renewal and recovery, as the water below is brought to the surface and cools. Surface renewal models provide expressions for the mean temperature difference across the TBL, $\Delta SST_{subskin} = SST_{subskin} - SST_{skin}$ [Liu *et al.*, 1979; Soloviev and Schlüssel, 1994]. The models are based on the notion of a statistical distribution of times between surface renewal events, with the mean time between renewals being the surface renewal timescale, τ . The random disruption of the TBL results in a distribution of skin temperatures, with the mean being SST_{skin} . Surface renewal theory is based on the assumption that the interface is completely renewed on each disruption, which has not been verified experimentally.

[4] High-resolution, low-noise IR cameras have provided new insight into the dynamic nature of the skin layer and the possibility of directly verifying that complete surface renewal occurs. If the interface is completely disrupted, then the distribution of temperatures in an IR image should include $SST_{subskin}$ and should provide a measure of $\Delta SST_{subskin}$. Furthermore, if complete disruption occurs for each renewal, then $\Delta SST_{subskin}$ should be comparable to the cooling that can occur in time τ (the mean time between renewals). Zappa *et al.* [1998] estimated $\Delta SST_{subskin}$ as the maximum difference across thermal wakes caused by wires disrupting the ocean skin layer. Garbe *et al.* [2004] measured $p(T_{skin})$, the probability density function (PDF) of T_{skin} , in the laboratory and computed $\Delta T_{subskin}$ by fitting a model function to the empirical $p(T_{skin})$. However, neither of these studies included radiometric measurements of sufficient accuracy to verify the validity of the approach.

[5] Here we present results from an experiment investigating the relationship between $p(T_{skin})$ and $T_{subskin}$ conducted in a wind-wave flume using a calibrated IR radiometer, an IR camera, a fast-response temperature profiler, and an air-side profiling system. To the best of our knowledge, this is the first laboratory experiment to combine accurate radiometric measurements of T_{skin} with measurements of $T_{subskin}$, $p(T_{skin})$, and the net heat flux, Q . We use this unique combination to determine, for the first time, if both complete and partial surface renewal occurs at a wind-forced air-water interface.

2. Experimental Procedure

[6] The experiment took place in the NASA Air-Sea Interaction Research Facility (NASIRF), which is a wind-wave flume located at the NASA Wallops Flight Facility. The NASIRF is 18.3 m long, 1.22 m high, 0.91 m wide, with water depth of 0.76 m, air headspace of 0.46 m, and

¹Applied Physics Laboratory, University of Washington, Seattle, Washington, USA.

²Department of Civil and Environmental Engineering, University of Alberta, Edmonton, Alberta, Canada.

³Lamont-Doherty Earth Observatory, Earth Institute at Columbia University, Palisades, New York, USA.

Table 1. Experimental Conditions and Results^a

Run	Experimental Conditions						Results					
	U (m s ⁻¹)	u_* (m s ⁻¹)	Q (W m ⁻²)	$\Delta T_{air-skin}$ (K)	RH (%)	$\Delta T_{subskin}$ (K)	ΔT_τ (K)	PR	τ (s)	t_* (s)	δ_l (mm)	
7	4.2	0.18	128	-2.8	70.4	0.15	0.06	99.92	0.56	2.60	0.28	
8	6.1	0.36	442	-6.0	71.0	0.19	0.14	99.99	0.24	0.37	0.18	
10	6.2	0.30	262	-3.1	71.9	0.13	0.10	99.83	0.33	0.51	0.22	
11	7.9	0.37	274	-2.7	72.6	0.16	0.08	99.98	0.24	0.63	0.18	
12	4.0	0.17	182	-3.6	73.4	0.14	0.09	99.65	0.56	1.20	0.28	
13	6.9	0.35	285	-2.6	74.2	0.18	0.10	99.98	0.33	0.76	0.22	
14	9.2	0.51	263	-2.1	75.0	0.13	0.08	99.94	0.21	0.51	0.17	
16	9.0	0.41	174	-2.3	75.6	0.17	0.05	99.98	0.20	1.84	0.17	
17	6.8	0.29	102	-1.6	76.3	0.20	0.03	99.98	0.22	7.73	0.18	
18	7.9	0.33	103	-2.4	76.7	0.13	0.03	99.90	0.21	2.99	0.17	
19	5.3	0.17	75	-2.7	76.9	0.15	0.03	99.97	0.42	8.19	0.24	
20	4.1	0.09	50	-3.9	77.2	0.15	0.02	99.86	0.63	18.68	0.30	
21	6.1	0.23	105	-3.0	77.5	0.10	0.04	99.38	0.36	1.73	0.23	
32	6.8	0.33	144	-2.8	78.3	0.16	0.05	99.97	0.29	2.39	0.20	
33	6.3	0.29	144	-2.9	79.1	0.14	0.05	99.88	0.32	1.99	0.21	
34	5.4	0.20	91	-3.0	79.6	0.18	0.04	99.99	0.40	7.92	0.24	
35	8.0	0.44	181	-2.0	80.1	0.12	0.05	99.88	0.21	0.84	0.17	
36	9.3	0.55	198	-1.8	80.7	0.10	0.05	99.71	0.19	0.48	0.16	
37	7.9	0.43	382	-7.9	81.1	0.24	0.09	100.0	0.15	0.77	0.15	
38	7.9	0.42	242	-4.5	79.7	0.22	0.06	100.0	0.16	1.66	0.15	
39	8.0	0.43	97	0.1	77.8	0.18	0.02	99.98	0.15	7.00	0.15	
41	8.0	0.44	20	3.9	75.8	0.13	0.01	99.95	0.21	81.64	0.17	

^aReference number *Run*, Wind Speed U , air-side friction velocity u_* , Net Upward Heat Flux Q , Air-Skin Temperature Difference $\Delta T_{air-skin}$, Relative Humidity RH , Subskin-Skin Temperature Difference $\Delta T_{subskin}$, Recovery Temperature Change ΔT_τ , Percentile Rank of $p(T_{skin})$ corresponding to $T_{subskin}$ PR , Renewal Time Scale τ , Recovery Time, t_* , and the Diffusive Length Scale δ_l .

provides control of air temperature, relative humidity, RH , and water temperature. Wind speed, U , was varied from 4.1 to 9.3 m s⁻¹, the bulk air-skin temperature difference ranged from -7.9 K to 3.9 K, and RH was between 70% and 81%. The data set consists of 22 5-min runs with air-side friction velocity, u_* , between 0.09 m s⁻¹ and 0.55 m s⁻¹, Q between 20 and 442 W m⁻² (upward), and $\Delta T_{subskin}$ between 0.10 K and 0.24 K. Table 1 lists conditions for each run and results presented below.

[7] Calibrated T_{skin} was provided by LabRad, an IR radiometer system based on the field system CIRIMS (Calibrated, Infrared, In situ Measurement System) [Jessup and Branch, 2008]. LabRad uses a thermally-stabilized IR thermometer (KT-15, Heitronics), which alternately views the water and a blackbody. The incidence angle was 50° and T_{skin} was corrected for reflections. The combination of thermal stabilization, on-going calibration, and reflection correction provided an accuracy of 0.05 K in the measurement of T_{skin} , which is better than the accuracy of 0.1°C reported for the CIRIMS because of the controlled laboratory conditions [Jessup and Branch, 2008].

[8] The $p(T_{skin})$ was measured using a longwave IR camera (640Q, AIM) mounted at an incidence angle of 25° at a distance of 1 m, resulting in an image size of approximately 0.90 m × 0.62 m (long dimension along the flume axis). The focal plane array of the IR camera has dimensions 640 × 512, which translates to an average pixel dimension of 1.4 mm × 1.2 mm. The sampling frame rate was 30 Hz and $p(T_{skin})$ was computed from the histogram of the pixel values over 1 min. The IR camera has a Noise Equivalent Temperature Difference of 20 mK and $p(T_{skin})$ was calibrated by assigning T_{skin} measured by LabRad to the mean of the distribution. The IR camera also was used in conjunction with a 25 W CO₂ laser to measure the surface renewal time scale, τ , using the Active Controlled Flux Technique, or ACFT [Atmane et al., 2004; Haußecker et al.,

1995]. In the ACFT, the IR camera is used to measure the temperature decay of a small patch of the water surface heated by the laser. The surface renewal time scale is estimated using a surface renewal model which incorporates an exponential decay of patch temperature.

[9] The calibrated $T_{subskin}$ was measured by combining a fast-response temperature profiling system with fixed, calibrated subsurface temperature sensors. The profiler measured the gradient between the depth of the accurate, fixed sensors and the variable free surface. The measurement system was designed such that the shallowest profiler measurement, when calibrated, is representative of $T_{subskin}$. (The system was not intended to measure the profile within the TBL as recently reported by Ward and Donelan [2006].) The profiler was a combined temperature and conductivity (T/C) probe (model 125, Precision Measurement Engineering) consisting of a FP07 thermistor and a fast conductivity sensor for detecting the free surface. The FP07 is a glass bead with a diameter of 2.2 mm and a minimum response time of 10 ms. The accuracy is ±0.050°C and the noise level from 10 Hz to 200 Hz is 0.006°C. The T/C sensor was mounted on an L-shaped frame attached to a linear actuator that moved the sensor from a depth of 150 mm through the surface at a maximum speed of 200 mm s⁻¹. The cycle time for a profile was approximately 4 s, which resulted in roughly 75 profiles for a typical 5-min run (only upward profiles were use).

[10] The free surface was detected using the conductivity time series and the average temperature profiles for each run were calibrated using two sensors (SBE-3, accuracy 0.001 K, Seabird) at depths of 28 mm and 72 mm (a third SBE-3 was located at 260 mm). The profile temperature just prior to the free surface detection was taken as $T_{subskin}$. Based on the probe characteristics and profiler speed, we estimate the depth of $T_{subskin}$ to be approximately 1 mm. For the results presented here, $\Delta T_{subskin} = T_{subskin} - T_{skin}$.

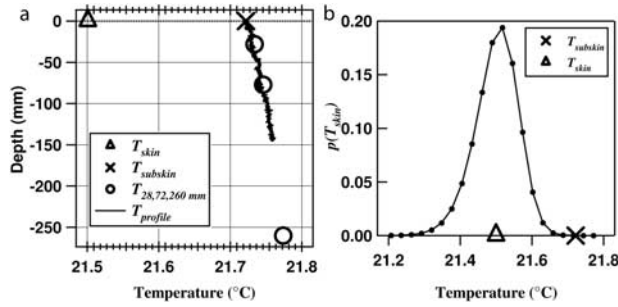


Figure 1. (a) Typical near surface temperature profile (Run 38, see Table 1), fixed-sensor temperatures (circles), $T_{subskin}$ from the profiler (X), and T_{skin} (triangle). (b) Probability Density Function (PDF) $p(T_{skin})$ corresponding to Figure 1a showing long tails both left and right. The PDF is calibrated by assigning T_{skin} (triangle) to the mean. $T_{subskin}$ (X) consistently occurs in the far right tail.

[11] The gradient flux technique [McGillis *et al.*, 2001] was used to measure the air-water fluxes of momentum and both latent and sensible heat. U was measured using two pitot tubes equipped with pressure transducers (264, Setra), one at a fixed height of 20 cm above the surface and a second that was profiled to measure u_* . Specific humidity was retrieved from RH and T_a measured using combined temperature/humidity sensors (HMP233/HMP45A, Vaisala) at the profiling and fixed locations. The net heat flux Q was taken as the sum of the latent, sensible, and radiative components.

3. Results and Discussion

[12] For each run, $p(T_{skin})$ was computed and the percentile rank corresponding to $T_{subskin}$ from the temperature profile was determined. A typical temperature profile is shown in Figure 1a along with $T_{subskin}$, T_{skin} , and the temperatures at fixed depth, T_{28mm} , T_{72mm} , T_{260mm} , where the subscript denotes the depth. The profile shows a temperature change of less than 0.04 K over a depth of roughly 150 mm and that the trend is consistent with all three fixed point-measurements. The difference between T_{28mm} and $T_{subskin}$ for all 22 runs remained less than 0.04 K, indicating that the near surface layer was well mixed. (An uncertainty in the measurement depth of O(1 mm) would introduce an error in $T_{subskin}$ of only O(10^{-4} K)). Figure 1b shows the corresponding $p(T_{skin})$, which is characterized by relatively long tails on both ends and is typical of all runs. Also shown in Figure 1b is T_{skin} (measured by LabRad and assigned to the mean of the distribution) and $T_{subskin}$, which consistently occurred in the far right tail. For 19 of 22 runs, the $T_{subskin}$ percentile rank was above 99.80 and for all runs the average percentile rank was 99.90. This result demonstrates that $T_{subskin}$ consistently corresponds to the maximum values within $p(T_{skin})$ and, consequently, that complete renewal of the TBL occurs.

[13] The finding that $T_{subskin}$ on average occurs at the 99.90 percentile also implies that SST_{skin} could be inferred by combining measurements of $p(SST_{skin})$ and $SST_{subskin}$ by calibrating $p(SST_{skin})$ with $SST_{subskin}$ rather than SST_{skin} (as done here). Relatively inexpensive uncooled IR cameras are now available that can provide adequate sensitivity to

measure $p(SST_{skin})$. Under nighttime or high wind conditions, the near surface layer is well mixed and thus $SST_{subskin}$ can be measured with a surface float. When a warm layer is present, $SST_{subskin}$ can be measured with a profiler [Ward *et al.*, 2004]. The combination of an IR camera and an appropriate *in situ* temperature sensor may provide an alternative to radiometric measurements of SST_{skin} , which remain challenging and limited [Donlon *et al.*, 2008; Jessup and Branch, 2008; Minnett *et al.*, 2001].

[14] While the occurrence of $T_{subskin}$ in $p(T_{skin})$ implies complete surface renewal, the consistently high percentile rank suggests that either there is very rapid cooling occurring if all renewal events are complete or that partial renewal also occurs. These interpretations can be evaluated by comparing $\Delta T_{subskin}$ to the expected cooling of a water parcel at the surface during the mean time between renewals, τ . If most renewal events completely disrupt the surface, then the amount of cooling occurring in time τ should be comparable to $\Delta T_{subskin}$. If the cooling in time τ is significantly less than $\Delta T_{subskin}$, then a significant number of renewal events must occur where the skin temperature does not reach $T_{subskin}$, implying that the TBL is only partially penetrated.

[15] The surface renewal time scale, τ , measured using ACFT is shown in Figure 2a as a function of u_* . This measurement can be compared to recent direct measurements of the TBL thickness, δ_c , from Ward and Donelan [2006] by reformulating τ in terms of a diffusion length scale, δ_l through $\delta_l = \sqrt{\kappa\tau}$, where κ is the thermal diffusivity. Figure 2b shows that δ_l and δ_c are of the same order of magnitude and have a similar dependence on u_* , which indicates that the ACFT-derived τ is a reasonable and consistent measure of the surface renewal time scale.

[16] If we assume that the temperature across the TBL is governed by molecular diffusion, the value of the temperature difference across the TBL at time t after complete disruption is given by [Soloviev and Schlüssel, 1994]

$$\Delta T(t) = 2\pi^{-1/2}(t/\kappa)^{1/2}q_0 \quad (1)$$

where $q_0 = Q/\rho c_p$, ρ is the density of water, and c_p is the specific heat of water at constant pressure. We used (1) to compute the recovery temperature change, ΔT_τ , for each run with $t = \tau$ and using the measured heat flux. We find

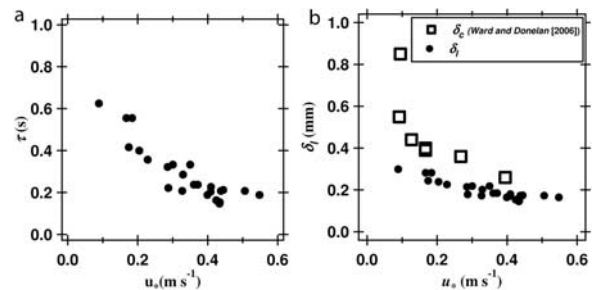


Figure 2. (a) Renewal time scale τ derived from the Active Controlled Flux Technique versus air-side friction velocity, u_* . (b) Conductive boundary layer thickness measured by Ward and Donelan [2006], δ_c , and diffusive length scale, δ_l (based on measured τ in Figure 2a) versus u_* .

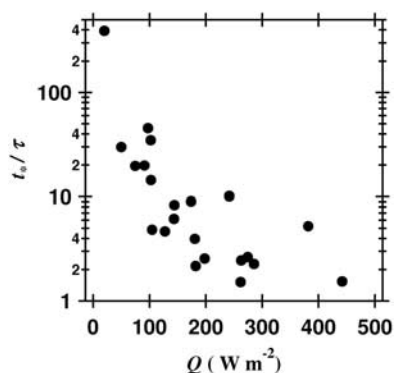


Figure 3. Ratio t^*/τ of the time required for a water parcel to cool to T_{skin} to the mean time between renewals versus heat flux Q (log-linear axes). The ratio approaches unity only for high heat flux, implying that the degree to which complete renewal occurs depends on the forcing.

$\Delta T_\tau = 0.06 \pm 0.03$ K (mean ± 1 s.d.) compared to the measured $\Delta T_{subskin} = 0.16 \pm 0.04$ K. That the mean $\Delta T_{subskin}$ is more than twice the mean ΔT_τ indicates that a water parcel that completely renews the surface would not have enough time, on average, to cool down to T_{skin} (the mean of $p(T_{skin})$) before the next renewal event.

[17] The finding that the cooling that occurs during the mean time between renewals is less than half of the mean temperature difference across the TBL implies that a significant fraction of renewal events only partially renew the TBL. The variability of the degree to which the TBL is completely renewed is provided by comparing τ to the time required for a water parcel at the surface to cool to the mean skin temperature, t^* , which we computed from (1) using the measured $\Delta T_{subskin}$. Figure 3 shows the ratio t^*/τ versus heat flux Q on log-linear axes. The ratio is much greater than unity for low heat flux and decreases towards unity with increasing heat flux. This result implies that the degree to which the TBL is completely renewed depends on the forcing, which is consistent with the finding by Zappa *et al.* [1998] that the restoring internal energy of the cool skin layer increases with heat flux and energy dissipation [see Zappa *et al.*, 1998, Figure 9]. Figure 3 also supports the hypothesis of Atmane *et al.* [2004] that conceptual models for air-water exchange based on the surface penetration concept [Harriott, 1962] are to be preferred over surface renewal models.

4. Conclusions

[18] The relationship between the sub-skin temperature, $T_{subskin}$, and the T_{skin} probability density function, $p(T_{skin})$, was examined using simultaneous measurements of T_{skin} , $T_{subskin}$, and $p(T_{skin})$ in a wind-wave flume. $T_{subskin}$ was measured with a combination of accurate fixed-depth temperature probes and a depth-profiling system using a fast-response temperature and conductivity probe. The average T_{skin} was measured using a calibrated IR radiometer and $p(T_{skin})$ was obtained from an IR camera. The surface renewal time scale, τ , was measured using the Active Controlled Flux Technique and the net heat flux and air-

side friction velocity were measured using the gradient flux technique. We found that $p(T_{skin})$ typically has significant tails and that $T_{subskin}$ consistently occurred in the extreme of the right hand tail. Specifically, the percentile rank of $p(T_{skin})$ that corresponded to $T_{subskin}$ was 99.80 or higher for 19 out of 22 cases and the average for all cases was 99.90. This result shows that $T_{subskin}$ corresponds to the maximum values in $p(T_{skin})$. It also suggests that T_{skin} can be measured using the combination of an IR camera and an *in situ* temperature sensor alone. The advent of inexpensive uncooled IR cameras makes this an alternative to the challenge of radiometric skin temperature measurements.

[19] The implication of the high percentile rank of $T_{subskin}$ in $p(T_{skin})$ for the degree to which complete surface renewal occurs was examined by comparing the expected cooling over the mean time between renewals, ΔT_τ , to the measured $\Delta T_{subskin}$. We found that the mean ΔT_τ of 0.06 K is less than half the mean $\Delta T_{subskin}$ of 0.16 K, which implies that a water parcel that completely renews the thermal boundary layer would not have sufficient time to cool down to the mean skin temperature, T_{skin} . It follows that a significant portion of renewal events only partially disrupts the thermal boundary layer. This conclusion is supported by the finding that the ratio of the time required for a water parcel to cool by $\Delta T_{subskin}$ to the mean time between renewals only approaches unity at high heat fluxes.

[20] Our results demonstrate, for the first time, that complete renewal of the thermal boundary at an air-water interface can occur under wind forcing. Furthermore, we infer that partial renewal is a common occurrence. Since complete disruption of the surface on every renewal is a fundamental assumption of surface renewal theory, this result should motivate further research into improving air-sea transfer models.

[21] **Acknowledgments.** We thank S. Long, R. Branch and T. Litchendorf. NSF grants OCE-9911320 and OCE-0425305 to ATJ and WEA, OCE-0425395 to CJZ, and CFCSA grant to MRL. We also acknowledge the comments of Kristina Katsaros in revising this manuscript.

References

- Atmane, M. A., et al. (2004), On the use of the active infrared technique to infer heat and gas transfer velocities at the air-water free surface, *J. Geophys. Res.*, *109*, C08S14, doi:10.1029/2003JC001805.
- Donlon, C. J., et al. (1999), Implications of the oceanic thermal skin temperature deviation at high wind speed, *Geophys. Res. Lett.*, *26*, 2505–2508, doi:10.1029/1999GL900547.
- Donlon, C. J., et al. (2002), Toward improved validation of satellite sea surface temperature measurements for climate research, *J. Clim.*, *15*, 353–369, doi:10.1175/1520-0442(2002)015<0353:TIVOSS>2.0.CO;2.
- Donlon, C., et al. (2008), An infrared sea surface temperature autonomous radiometer (ISAR) for deployment aboard volunteer observing ships (VOS), *J. Atmos. Oceanic Technol.*, *25*(1), 93–113, doi:10.1175/2007JTECH0505.1.
- Fairall, C. W., et al. (1996), Cool-skin and warm-layer effects on sea surface temperature, *J. Geophys. Res.*, *101*, 1295–1308, doi:10.1029/95JC03190.
- Garbe, C., et al. (2004), A surface renewal model to analyze infrared image sequences of the ocean surface for the study of air-sea heat and gas exchange, *J. Geophys. Res.*, *109*, C08S15, doi:10.1029/2003JC001802.
- GHRSS-PP (2005), The recommended GHRSS-PP data processing specification GDS, report of the GODAE High Resolution Sea Surface Temperature Pilot Project, Met Office, Exeter, UK.
- Harriott, P. (1962), A random eddy modification of the penetration theory, *Chem. Eng. Sci.*, *17*, 149–154, doi:10.1016/0009-2509(62)80026-8.
- Haußecker, H., et al. (1995), Heat as a proxy tracer for gas exchange measurements in the field: principles and technical realization, in *Air-Water Gas Transfer*, edited by B. Jähne and E. C. Monahan, pp. 405–413, Aeon, Hanau, Germany.

- Jessup, A. T., and R. Branch (2008), Integrated ocean skin and bulk temperature measurements using the Calibrated Infrared In Situ Measurement System (CIRIMS) and through-hull Ports, *J. Atmos. Oceanic Technol.*, *25*, 579–597, doi:10.1175/2007JTECHO479.1.
- Katsaros, K. B. (1980), The aqueous thermal boundary layer, *Boundary Layer Meteorol.*, *18*, 107–127, doi:10.1007/BF00117914.
- Liu, W. T., et al. (1979), Bulk parameterization of air-sea exchanges of heat and water vapor including molecular constraints at the interface, *J. Atmos. Sci.*, *36*, 1722–1735, doi:10.1175/1520-0469(1979)036<1722:BPOASE>2.0.CO;2.
- McGillis, W. R., et al. (2001), Carbon dioxide flux techniques performed during GasEx-98, *Mar. Chem.*, *75*, 267–280, doi:10.1016/S0304-4203(01)00042-1.
- Minnett, P., et al. (2001), The Marine-Atmospheric Emitted Radiance Interferometer (M-AERI), a high-accuracy, sea-going infrared spectroradiometer, *J. Atmos. Oceanic Technol.*, *18*, 994–1013, doi:10.1175/1520-0426(2001)018<0994:TMAERI>2.0.CO;2.
- Soloviev, A. V., and P. Schlüssel (1994), Parameterization of the cool skin of the ocean and the air-ocean gas transfer on the basis of modeling surface renewal, *J. Phys. Oceanogr.*, *24*, 1339–1346, doi:10.1175/1520-0485(1994)024<1339:POTCSO>2.0.CO;2.
- Ward, B. (2006), Near-surface ocean temperature, *J. Geophys. Res.*, *111*, C02004, doi:10.1029/2004JC002689.
- Ward, B., and M. Donelan (2006), Thermometric measurements of the molecular sublayer at the air-water interface, *Geophys. Res. Lett.*, *33*, L07605, doi:10.1029/2005GL024769.
- Ward, B., R. Wanninkhof, P. J. Minnett, and M. J. Head (2004), SkinDeEP: A profiling instrument for upper-decameter sea surface measurements, *J. Atmos. Oceanic Technol.*, *21*, 207–222, doi:10.1175/1520-0426(2004)021<0207:SAPIFU>2.0.CO;2.
- Zappa, C. J., et al. (1998), Skin layer recovery of free-surface wakes: Relationship to surface renewal and dependence on heat flux and back-ground turbulence, *J. Geophys. Res.*, *103*, 21,711–21,721, 722, doi:10.1029/98JC01942.
-
- W. E. Asher, A. T. Jessup, and K. Phadnis, Applied Physics Laboratory, University of Washington, 1013 NE 40th Street, Seattle, WA 98105-6698, USA. (jessup@apl.washington.edu)
- M. Atmane and M. R. Loewen, Department of Civil and Environmental Engineering, University of Alberta, Edmonton, AB T6G 2W2, Canada.
- C. J. Zappa, Lamont-Doherty Earth Observatory, Earth Institute at Columbia University, 61 Route 9W, Palisades, NY 10964, USA.